NATIONAL ADVISORY COMMITTEE FOR AERONAUTICS

TECHNICAL MEMORANDUM 1331

INVESTIGATIONS OF THE BOUNDARY-LAYER CONTROL ON A FULL SCALE SWEPT WING WITH AIR BLED OFF FROM THE TURBOJET

By P. Rebuffet and Ph. Poisson-Quinton

Translation of "Recherches sur l'Hypersustentation d'une Aile en Flèche Réelle par Controle de la Couche Limite Utilisant le Prélèvement d'Air sur le Turbo-Réacteur." la Recherche Aéronautique, O.N.E.R.A., No. 14, March-April, 1950.

Washington
April 1952

NATIONAL ADVISORY COMMITTEE FOR AERONAUTICS

TECHNICAL MEMORANDUM 1331

INVESTIGATIONS OF THE BOUNDARY-LAYER CONTROL ON A FULL SCALE SWEPT WING WITH AIR BLED OFF FROM THE TURBOJET*

By P. Rebuffet and Ph. Poisson-Quinton

SUMMARY

The following account reviews the various stages of a research program relative to the high-lift devices on a swept wing by combined suction and blowing (jet action), with ejectors fed by air bled off (extracted) from the turbojet.

After reviewing the essential principles of the boundary-layer control obtained by comparison with theory, the electric analogies and the wind-tunnel tests as well as the essential elements of ejector operations, the writers describe the tests made in the large tunnel at Chalais-Meudon on a full-scale model of the SO 6020 wing.

They comment on some results relative to take-off and landing and examine the airplane-turbojet energy balance.

The writers emphasize that this investigation has been carried out in a remarkable spirit of teamwork and particularly their chief collaborators Messrs. Mirande and Ravailhe, Jousserandot and Chevallier.

They have also drawn on the unpublished reports of Messrs. Lebrun, Legras, Nieviaski, Pontezière of the O.N.E.R.A. and of Mr. Chiaffiote of the Hispano-Suiza Company.

NOTATION

S	reference area
V_0	speed at infinity

*"Recherches sur l'Hypersustentation d'une Aile en Flèche Réelle par Controle de la Couche Limite Utilisant le Prélèvement d'Air sur le Turbo-Réacteur." la Recherche Aéronautique, O.N.E.R.A., No. 14, March-April, 1950, pp. 39-54.

s width of blowing slot

l local chord

I geometric incidence

i aerodynamic incidence

q_v, q_m, q_p flow volume, flow mass, and flow weight

V_a mean speed of suction flow tube coefficient of flow $C_q = \frac{q_v}{SV_0}$ (expanded to 15° C, 760 mm of mercury)

C_q', C_q'', C_q flow coefficient of injection suction and blowing

C_μ momentum flow coefficient $\frac{q_m}{\frac{\rho}{2}S}\frac{V_s}{V_0^2}$

$$\lambda = \frac{\text{area of mixer cross section}}{\text{area of injector cross section}} = \frac{S_m}{S'}$$

$$\alpha = \frac{\text{area of diffuser outlet section}}{\text{area of mixer section}} = \frac{S}{S_m}$$

$$\frac{L}{D} = \frac{\text{length of mixer (circular ejector)}}{\text{diameter of mixer}}$$

$$\mu = \frac{\text{mass flow of suction fluid}}{\text{mass flow of engine fluid}} = \frac{q''_m}{q'_m}$$

$$g = \frac{\text{momentum flow at blowing slot}}{\text{momentum flow at ejector}} = \frac{q_m}{q'_m}\frac{V}{V'}$$

$$e = \frac{\text{flow of kinetic energy at blowing slot}}{\text{flow of kinetic energy of engine jet}} = \frac{q_m}{q'_m}\frac{V^2}{V'^2}$$

INTRODUCTION

The airfoils suitable at sonic speeds are generally characterized by a low $C_{z_{max}}$, which is still further reduced by the sweptback form of the wing.

These two factors led to the study of high-lift devices designed to develop high C_z on modern high-speed aircraft, to improve the landing as well as the take-off.

The control of the boundary layer responsible for the separation of flow and the limitation of C_z has been studied for a long time on thick airfoils, without combining the suction or the jet action with a modification of the airfoil camber. The power involved and the flows (suction or blowing) were considerable.

Numerous technical studies have been made especially by the Germans (ref. 1) during the war, on more suitable airfoils and with partial-span flaps; some were flight-tested.

In France, certain airplane firms included in their research program on high-lift devices, the study of suction or jet action, and it was proposed to combine the two methods by utilizing injectors. The S.N.C.A.S.O. had considered, since 1946, the construction of a scale model of the large tunnel at Chalais-Meudon, for the SO 6008 bis airfoil.

The jet airplane affords, moreover, a new possibility of boundary-layer control by suction or by jet action (blowing).

The first solution has been the subject of several studies (refs. 2, 3), the second, more recently, was tested by the Hispano-Suiza firm.

The aerodynamical department of the O.N.E.R.A. has, since 1946, correlated the research data on boundary-layer control, checked the wind-tunnel data against those obtained in potential flow by electric analogy, and made a theoretical study of the effect of sinks (suction).

These two comparisons made it possible to orientate the experimental investigations, since the purpose of the boundary-layer control is to assure a potential flow under certain provisions to be specified later on.

These basic researches had to be made on a Chalais-Meudon mock-up which permitted:

Operation at a Reynolds number near that at landing, the mock-up having the dimensions of a flying airplane

Testing of components at full scale

Allowance for certain number of contingencies imposed by a product similar to that of a real airplane

It was advisable to make this study on a concrete case. The earlier projects of the S.N.C.A.S.O. were computible with the program of the O.N.E.R.A., the control devices were applied to a swept wing model of the SO 6020 type. Besides, bleeding off air from the turbojet made it possible to reproduce at Chalais-Meudon, the image of the airplane, by dissociating first the airplane from the turbojet, which was installed outside of the tunnel, thus, assuming a safer operation as well as a more accurate way of recording the drag, that was to be determined simultaneously with the lift.

It was, nevertheless, possible to measure the thrust of the jet, with due regard to the air bleeding from the turbojet.

The study at Chalais-Meudon had to be made in competition with the O.N.E.R.A. through:

The S.T.A., engine section which had put the Nene Hispano-Suiza turbojet at the disposal of the O.N.E.R.A.

The Arsenal de l'Aéronautique, which had lent the turbojet support frame and the corresponding control cabin

The Hispano-Suiza Company that constructed the collector for the air bleed and assumed the control of the turbojet for the duration of the tests

The S.N.C.A.S.O. which, manufactured the model at the request of the O.N.E.R.A. and made the study and perfected it

Lastly, the airplane section of the S.T.A. which underwrote the tests Chalais-Meudon

About 45 to 50 men were involved in this undertaking, which included:

514 polars and pitching moments
2000 hinge moments
31500 pressure measurements on the wing (700 pressure gage negatives)
850 photographs
speed and temperature measurements

PRINCIPLES AND APPLICATION OF BOUNDARY-LAYER CONTROL BY HIGH-LIFT DEVICES

Of the multitude of systematic studies by the O.N.E.R.A. on this subject (ref. 4) simple guiding ideas can be enumerated:

It is known that the maximum lift of an airfoil is limited by the break away of the boundary layer from the upper surface. This separation has its origin in the appearance of a pressure gradient and is accentuated with the incidence or with the deflection of a flap. The remedy is to reduce the peaks of the speed increase by acting on the curvature of the center line of the profile or else to prevent or limit this separation by controlling the boundary layer.

In the first method, the fluid is assumed perfect and yields an incurved profile center line, in a kind of downward deflection of several flaps, hinged front and rear.

The Pérès-Malavard electric analogy method affords a very fruitful study of the best distribution of the increase of speed over the upper surface of an airfoil; for a given lift coefficient, it is possible to increase the camber of the mean line for distributing the peaks of the speed increase accompanying each variation incurvative due to the flap setting.

The most dangerous increase, which appears at the leading edge can be reduced by a deflection of the latter which puts the stagnation point back at the nose of the airfoil. This deflection must be such that the increase at the nose and the droop are of the same order of magnitude.

In viscous fluid the maximum lift is limited by the separation downstream from the peaks; it can be remedied by boundary-layer control either by suction or blowing. Both methods have a secondary effect on the circulation around the airfoil: source effect for suction which is theoretically calculable, or the induction effect for blowing. It has been shown that the lift increase was proportional, respectively, to the induced flow and to the momentum flow. This secondary effect, negligible as long as the fluid is separated, remains apparent only after elimination of the separation. In other words, plotting the lift increase ΔC_z against the flow parameter C_q or the momentum C_μ, yields a curve with asymptotic direction from the critical flow assuming the readherence of the boundary layer. Above this value, the profile can be regarded as functioning in perfect fluid for which the laws (ΔC_z, flow) are linear. Experience indicates that it is not important to exceed the readherence flow from the energy point of view, because the lift increases only very little.

The first wind-tunnel test was made on wings with drooped nose fitted with flaps and slotted suction or blowing slots in the droop. Experience has proved the efficiency of the boundary-layer control for obtaining readherence, the maximum lift being no longer limited except by the separation at the leading edge.

The applications are difficult owing to the over-all dimensions of the suction or blowing channels and to the practical impossibility of mounting auxiliary compressors in the airplane. To make it practicable, it is necessary to utilize a part of the engine power installed on the airplane and to reduce the dimensions of the air ducts along the span.

This is the reason why our studies on the application of boundary-layer control were oriented from the beginning toward the employment of compressed air, making it possible to distribute the blast along the wing span through a small size duct supplied by air drawn from the compressor of the turbojet.

The compressed air can be expanded directly in a blowing slot but this method poses problems difficult to solve: discontinuity of stressed skin covering at the upper surface, control of the width of a very fine slot before being rigid, and especially the correct distribution of the flow along the wing span.

Lastly, the ejector, in spite of its low energy efficiency, has the advantage of simplifying the wing structure considerably and at the same time assuming the boundary-layer control by suction followed by blowing at two points of the profile.

EFECTORS

Definitions

In general, an ejector (fig. 1) consists of:

An injector supplying the "primary air" characterized by the velocity head p' (dynamic pressure)

A suction chamber and suction cone where the sucked or "secondary" air enters

A mixer whose speed and temperature are equalized

A diffuser terminating at the blowing slot

It is characterized by the geometric parameters λ and α; its aerodynamic functioning is defined by μ, g, and e.

Ejectors have been studied in static tests as well as on airfoils in wind tunnels for a long time. It is conceded that the static pressure existing on the profile at the location of the suction and jet action are similar, the functioning of ejectors is the same with or without flow past the profile, this remark justifies the static tests.

The jet velocities have, for the utilization of ejectors, as far as the boundary-layer control device is concerned, as much significance as the suction volume; in such ejectors the operating conditions differ considerably from the classical.

Tests

The theoretical study and the tests involved several types of ejectors: an ejector with flat mixer, without diffuser and a set of ejectors with circular mixer terminating in a diffuser, the section of which was developed from a circle to a rectangle (fig. 1).

The parameter λ can be varied by changing the section of the mixer or by varying the section and the number of injectors; the parameter α by modifying the mixer or the diffuser. The effect of the mixer length L and that of the variation of the loss of lead due to suction was studied at the same time.

The comparison of the two types of ejectors was extended to the coefficient of discharge μ, the speed of the blowing jet V_s, and the ratio of the momentum g. The results prove the identity of the functioning of the flat and circular ejectors.

The choice between the two solutions can be guided by considerations of size, weight, and facility of construction.

The circular ejectors favor high values of λ; values that give high discharge μ but a low momentum ratio g, with blowing slots of little thickness, because the section of the mixture does not occupy the entire span of the wing.

The flat ejectors with flat injectors simplify the design, but produce only small values of λ for these straight slots, hence a low μ, but a high g.

The best solution therefore seems to lie in a combination of ejectors with flat mixers and multiple circular injectors, so as to obtain high λ values for straight blowing slots.

Arrangements Adopted at Chalais-Meudon

The arrangements and the dimensions of the ejectors for the model of the SO 6020 airplane used in the large wind tunnel at Chalais-Meudon was determined in the light of these tests. It was finally decided to adopt multipler circular ejectors with the following characteristics:

$$\lambda \cong 28 \qquad \alpha \cong 0.75 \qquad \frac{L}{D} \cong 5$$

Figure 2 defines the development of the curves μ, g, e as functions of the injection pressure p'. A brief study of this graph shows that the induced flow is about $2\frac{1}{2}$ times that of the injected flow, that the momentum flow at the injector exit is sensibly maintained, but that the ratio of the kinetic energies is relatively small, of the order of 20 percent.

In the range of operations customary at Chalais-Meudon, the injection pressure p' is such that the speed in the throat of the injectors is sonic.

The characteristic coefficients μ, g, and e depend, to some extent, on the loss of lead at suction and, consequently, on the setting.

At $g = 0.8$ for the straight slot corresponding to $\alpha_1 = 0$, g reaches in effect, unity for the $\alpha_1 = 15$ setting.

It is quite evident that it is important to design the suction slot correctly in order to obtain correspondingly minimum loss of lead.

Exploration of Blowing Jet on a Flap of the Wing SO 6020

In this study the injectors were supplied by compressed air for the purpose of ascertaining the velocity distribution in the blowing jet.

In the case of the circular ejectors, figure 3 shows at 100 mm downstream from the blowing slot a regular distribution in span already, although with a slight fluctuation attached to each ejector.

This distribution is still more uniform when using an ejector with flat mixer and circular injectors, of a total section equal to that of the preceding arrangement but having twice the number of injectors.

Figure 4 shows the velocity profile of the blowing jet in the axis of an ejector or injector 100 mm downstream from the blowing slot.

TESTS ON A METAL MODEL IN TWO-DIMENSIONAL FLOW

Before making the tests on the full-scale model in the large tunnel at Chalais-Meudon, a very complete study was made on a SO 6008 bis, metal airfoil of 0.838-m chord, 1-m span, equipped with ejectors (fig. 5). According to a static test for defining the ejector characteristics, followed by a test between panels in the wind tunnel at Porte d'Issy, this wing element showed very promising results from the point of view of high-lift devices for landing and take-off.

The pressure distributions measured on the profile have been compared with those obtained in the electric tank (fig. 6).

The identity of the curves assumes that the separations are completely reabsorbed by blowing, while this is not the case for high settings. Moreover, suction and blowing introduce a secondary effect of sinks and induction that was not represented in the theoretical study. It follows a different chordwise load distribution for an identical lift.

Figure 7 refers to the following configuration:

leading edge setting $\eta = 30^\circ$

first suction flap $\alpha_1 = 25^\circ$

second blowing flap $\alpha_2 = 45^\circ$

which are marked 30 B-25-45°, the letter B indicates that the leading-edge slot is plugged.

At constant incidence the readherence of the boundary layer to the first and second flap is manifested by a sudden increase in C_z; beyond the flow of readherence the linear law (C_z, C_μ) prevails, which corresponds to the action on the potential flow.

The unit curves (C_z, i) undergo a translation of the ordinates with increasing C_μ, but it seems that the incidence of $C_{z_{max}}$ decreases as a result of the stalling of the leading edge which proceeds from a critical value of the maximum speed increase connected with the leading-edge radius.

A series of tests was run on this wing element with varying leading-edge radius.

For a given contour, the stall produced for a given C_z is so increased considerably as the leading-edge radius is increased. The analysis of the pressure distributions shows the great increase of admissible critical speed increases, when the radius increases.

The solution of the combined flat mixer and multiple circular injectors was recently attempted on the metal wing element SO 6008 bis.

The model was tested in the wind tunnel at Cannes. According to the first results obtained, there is a net improvement of C_μ (of the order of 30 percent), which is manifested by a more effective control of the boundary layer.

The practical construction of flat mixers reveals itself, as predicted, much easier than that of multiple circular ejectors.

THE SO 6020 MODEL AT CHALAIS-MEUDON

The 10-percent thick wings copy the outside form of those of the SO 6020; they are joined to a fuselage, modified only in the front and rear parts, the length of the actual fuselage being unsuitable for the wind tunnel.

The construction is of wood, but with due regard to the placement of the essential components of the real wing structure.

The wing has an adjustable leading edge and two flaps (fig. 10), the setting α_1 is controlled by electric jets and measured by teledynes.

Cemented strain gages afforded the over-all measurement of the hinge moment of the flaps $\alpha_1 + \alpha_2$.

A series of static pressure orifices was installed in the section AB (fig. 8). Exploratory graphing hooks of the boundary layer are arranged at both sides of slot α_1 and in the blowing jet α_2. The wool streamers on one wing enabled the flow to be checked, and in particular to follow the readherence on the different parts.

Compressed Air for Model

The turbojet is housed with its control cabin outside of the wind tunnel (fig. 11). The air is bled off through special pipes which deflect a part of the flow feeding the combustion chambers (fig. 12) and terminate in a double collector.

The air enters the model through a symmetrical circuit (fig. 8) without introducing momentum, with insertions of flexible elements, that cause no stress at the wind-tunnel balance.

At entry in the model, a special joint enables variations of the incidences without vitiating the measurement of the pitching moment.

The characteristics p', T' of the fluid (sensibly at rest) before being distributed to the injectors spaced along the span, and also the total flow injected, q'_p, are measured.

In all tests the temperature T' is about 50° C, whereas, during bleeding off it may reach 200° C. For equal mass flow, the speed of ejection and hence the momentum flow is therefore much similar. The experimental results must be corrected for application to the airplane.

Functioning of the Turbojet

Figure 13, made at the Hispano-Suiza test stand, shows the evolution of the principal characteristics of the turbojet plotted against the pressure and the flow bleed-off weight.

The tests at Chalais-Meudon were carried out by varying the speed of the turbojet between 6000 and 11,600 rpm. The experimental points corresponding to three speeds are shown on the graph, they are situated on a straight line defined by the total section of the injectors.

The diagram contains the network of constant rotational velocities and bleed-off temperatures, the isotemperatures in the nozzle (after the turbine) and, in particular, that which limits the diagram to its upper part. The isothrust curves of the turbojet also included, involve the heat balance.

Procedure of Test

For a given geometrical form of the model, at an incidence I and a tunnel speed V_0, the inlet pressure at the injectors (and consequently the primary flow of the ejectors) were varied by changing the speed of the turbojet. The airspeed V_0 was varied between 18 m/sec and 35 m/sec $\left(3 \times 10^6 < Re < 6 \times 10^6\right)$.

To each injected flow q'_p, there corresponds a secondary flow $\mu q'_p$ which is none other than the flow sucked through the slot α_1; the total flow $(1 + \mu)q'_p$ is ejected by the blowing slot α_2. The momentum flow is decreased and from it the parameter C_μ.

The balance measures the three components of the resultant; the elements necessary for the calculation of the pitching moments, hinge moments, and pressure distributions are indicated; the observation and the wool tuft photographs are extremely instructive.

Reference Area

For computing the lift and drag coefficients, the wing area affected by the boundary-layer control was chosen, as it affords a much easier comparison with the tests in two-dimensional flow.

RESULTS OF TESTS

Representative Parameters of the Aerodynamic Phenomena

Suction and blowing induce flow changes at the wing which are manifested by lift and drag changes.

Lift.- Boundary-layer control makes it possible to make the flaps more efficient, and hence to increase the lift considerably. Moreover, the suction entails an increase in circulation resulting in a $\Delta C_z = K. \Delta C_q''$, the coefficient K being considerably higher as the suction slot at the upper surface is nearer to the trailing edge. In our specific case (slot at 57.5 percent from leading edge), this coefficient, given by the theory, is very low ($K = 2.38$) and the gain in lift is practically negligible for the flows involved $\left(C_q'' \ll \frac{1}{100}\right)$. By contrast the rise in the circulation by the induction of the blowing jet entails a considerable increase in the lift $\Delta C_z = K' \Delta C_\mu$; the coefficient K' likewise increases when the jet approaches the trailing edge, but it cannot be defined theoretically; the effect of blowing being preponderate, it is reasonable to represent the evolution of C_z as function of the jet action parameter C_μ.

Drag.- The suction-blowing combination must be considered: A certain mass of fluid q''_m is sucked in at a mean speed V_a (it can be obtained by measuring the velocity distributions above the lip (or rim) upstream from the slot); a mass q_m is ejected through the blowing slot at a speed V_s.

At low incidences for which the speeds V_s and V_a can be considered identical with their projections on the speed at infinity V_0, we obtain a force

$$-R_x = q_m V_s - q''_m V_a = \left[(1 + \mu)V_s - V_a\right] q''_m$$

$$= \left[V_s - \frac{V_a}{(1 + \mu)}\right] q_m$$

in the absence of an exact measurement of V_a, it can be estimated equal to V_0 with due allowance for the local increase of speed at this position (fig. 14), on the other hand, the $V_s \sim 4V_0$ and $\mu \cong 3$. The subtractive term is thus very small and is neglected.

Hence

$$-C_x = \frac{q_m V_s}{\frac{1}{2}\rho S V_0^2} = \frac{2C_q^2}{s/l} = C_\mu$$

s/l being the relative width of the blowing slot. The drag curves are likewise plotted against C_μ, which has been computed from C_q' by

$$C_\mu = \frac{2C_q'^2(1 + \mu)^2}{s/l}$$

with due amount of the variation of μ with the pressure.

Velocity distribution near the suction and blowing slots.- Figure 14 shows by way of example a velocity distribution upstream and downstream from the suction slot as well as downstream from the blowing slot, for several values of C_μ; the boundary layer upstream from the first slot is little affected by the suction, and completely suppressed downstream from it, the pocket of the speeds of the blowing jet indicates, on the other hand, that the induction effect accelerates the fluid well above the jet itself.

Mechanism of Readherence of Boundary Layer

It is interesting to follow the successive stages of readherence of the flow over the rear part of a wing for a specific configuration of flaps: nose not drooped, first slot suction $\alpha_1 = 25^\circ$, second slot blowing, $\alpha_2 = 45^\circ$, incidence $I = 12^\circ$.

The pressure distributions recorded in the section AB are shown in figure 15, the visualization of the flow by wool tufts in figure 16, and the lift curve ($I = 12^\circ$) as function of C_μ in figure 17. For $C_\mu = 0$, the two flaps have completely separated (phase a). The first flap readheres rather quickly when suction begins, while the flow is still severely agitated over the second flap ($100\ C_\mu = 1.3$, phase b); nevertheless, the increment of the lift is appreciable.

In the next phase (c), corresponding to $100\ C_\mu = 5.5$, the flow has completely separated from the two flaps. The orientation of wool tufts indicates the complete suppression of the oblique flow toward the tip of the sweptback wing. These different phases are manifested in the pressure distribution by a marked increase of speed over the rear part of the profile, which tend toward the theoretical increases of speed, whereas the correlative increase of circulation entails an increase in the speed at the leading edge. If the flow is increased further, there comes a moment where the circulation is such that the maximum increase at the leading edge exceeds the critical value and induces separation. In this phase (d), the lift increases is no longer linear and the curve (C_z, C_μ) bends inward. When the separation from the wing is generalized ($I = 15^\circ$ and over), another lift increase due to the action on the potential flow and the component of the blowing momentum for increasing flows, is observed.

The formation of the total drag as function of C_μ is also represented in figure 17; it increases with C_μ as a result of the increased induced drag.

If the latter is curtailed, the curves, for which the flow is sound, are sensibly reduced to a unique curve the mean slope of which is that of the theory ($-C_x = +C_\mu$).

Figure 18 shows that the readherence for the C_μ is considerably greater as the profile curvature is more pronounced; nevertheless, all curves tend toward one asymptotic direction.

A drooped nose reduces the speed increase at the nose as seen from the pressure distributions of figure 19. Its effect on $C_{z_{max}}$ is discussed later.

Cruising Configuration

The static tests proved that the aerodynamic resultant is equal to the blowing momentum; this roughly checks with the result obtained in the study of ejectors.

The same property is again verified with relative wind as seen in figure 20, where the setting of the polars is sensibly equal to C_μ at incidences for which the flow, without boundary-layer control, remains sound.

With boundary-layer control, the polars are sensibly parallel to the induced polar, although the latter is computed by the classical method of Prandtl, not applicable rigorously, to a swept wing.

Take-Off Configuration

Different configurations with moderate flap settings are designed for use at take-off. Certain forms are to be discarded for a specific take-off speed, be it that they do not furnish the corresponding C_z, or give an incidence too close to separation or give rise to abnormally high drag. A range of take-off C_z is established for seeking the best forms chosen by the minimum $(C_x - C_{xi})$. Figure 21 shows the corresponding network; it is apparent that high C_z necessitate a more pronounced setting.

Figure 22 compares the drag of different forms at constant C_z and variable α_2. The $C_x = f(\alpha_2)$ at the right for $C_\mu = 0$ and $100\ C_\mu = 5$ is shown by way of example.

For $\alpha_2 = 0$, the gain in C_x is greater than C_μ, and remains substantially the same when α_2 varies.

Landing

The influence of the three elements that define the profile camber is decomposed, in order to obtain the best $C_{z_{max}}$.

In the study of the effect of the drooped nose, the continuity of the profile was reestablished by an appropriate setting. Figure 23 shows the role of the drooped nose which, by reducing the speed increase at the nose, delays the separation and consequently lengthens the unit curves $C_z = f(i)$.

The best setting η lies between 15° and 30°. A study was made also on a drooped nose the suction being assured through the wing by ejectors in similar manner to the suction on flap α_1, whose slot was then closed (fig. 10).

It could be observed at this occasion that the flap α_1 overcame the separation, even for a setting of 25°, by induction of the blowing jet.

The suction in the droop of the nose, by impeding the separation from the forward part of the wing, postpones the incidence of $C_{z_{max}}$ a little too.

Varying only α_1, the best setting increases with C_μ, owing to the prevented separation due to the suction, according to the curves of figure 24.

The effect of the blowing flap α_2 (fig. 25) shows that the optimum is near 40° or 45°, depending on the values of C_μ.

In addition, $\frac{dC_z}{d\alpha_2}$ increases considerably with C_μ; this factor is favorable for assuming the lateral control by blowing aileron.

For a contour of primary interest from the point of view of landing it is advisable to take the total drag that corresponds to $C_{z_{max}}$ for several C_μ into consideration.

Figure 26 gives by way of example the polars obtained for the configuration 30 B-25-45°. The rise in C_z is substantial, especially for a swept wing with thin profile. Correlatively, the very significant drags are due in a large measure, to the induced drag.

Pitching Moments and Hinge Moments

Pitching moments.- One difficulty accompanying the use of high-lift devices is the correlative appearance of a high pitching moment. The equilibrium of the airplane necessitates an appreciable elevator setting which becomes strikingly nonlifting and reduces the $C_{z_{max}}$ of the airplane to the same extent.

The tests made at Chalais-Meudon on a model without empennage do not permit a direct treatment of the problem.

The O.N.E.R.A. has recently begun a series of studies in the wind tunnel at Cannes, on a complete airplane model equipped with drooped nose and blowing flap. The first results indicated that polars balanced up to C_z of the order of 4 are obtainable without having to change the initial setting of the tail.

Incidentally, it is noted that the blowing effects are favorable on the tail that is in a sound flow and highly deflected; the only limitation is the stalling over the tail.

Hinge moments.- The flaps α_1 and α_2 are constructed in four elements distributed along the span of a semispan wing (fig. 8). The hinge-moment measurement of α_1 and α_2 results in the following:

For the contour 30 B-25-45° taken as example, the hinge moment decreases 30 percent from root to tip, when the control of the boundary is inactive.

The improvement of the flow over the suction and blowing flaps, multiplies the initial hinge moment by a factor varying from 2 to 3.5, from root to tip. This confirms the qualitative conclusions drawn from the wool tuft observations, particularly in the case of swept wing.

The hinge moment does not change much with the incidence, even a little beyond $C_{z_{max}}$, an element favorable for lateral control.

For a nondrooped nose, the hinge moments start to decrease before $C_{z_{max}}$, even with boundary-layer control; this confirms the significance of adopting a drooped nose.

As to the forces required for flap control, they do not seem to pose particular structural problems.

BALANCE AIRPLANE TURBOJET

General

Bleeding off air from the turbojet limits its thrust as a result of the increased temperature upstream from the turbine. It must be allowed for in the performance determinations.

By contrast, the decrease in thrust for a given turbojet speed is negligible as shown in figure 13, while the specific consumption increases a little during the short period of bleed-off.

The preliminary study of ejectors and the over-all results pointed out previously have brought into evidence a relationship between the injected and blown momentums.

Consequently, with the employed notations

$$q'_m V' = g q_m V_s = g C_\mu \frac{\rho}{2} S V_0^2$$

The aerodynamic study defining C_μ, the weight and the C_z defining V_0, the term $q'_m V'$ supplied by the turbojet, is deduced. It is important to locate the corresponding points of operation on the bleeding-off diagram.

To this end, a net of curves of equal $q'_m V'$ can be plotted on the chart from which the equivalent surface of the injectors is then deduced.

Landing

By way of example, for a specified landing speed of 45 m/sec and operation at $100\ C_\mu = 10$, we get $q'_m V' = 266$; on the extrapolated diagram of the turbojet, the maximum thrust limited by the temperature, is 1780 kg equal to $C_x = 0.67$; if the airplane C_x is higher, the permanent flight is slightly lower; for the usual wing loading, the rate of descent is not more than 1 to 2 m/sec. The diagram also shows that the injector exit should be considerably increased.

Take-Off

The adaptation to an optimum configuration is obtained by a similar process: for a specified $C_z = 1.75$, the configuration is OB-15-15 (fig. 21); the maximum climb is reached with $100\ C_\mu = 2.5$, the corresponding drag is balanced by a thrust $P = 1028$ kg; the excess thrust ($\Delta P = 2190 - 1028$) makes it possible to obtain the rate of climb.

The diagram shows the ejection section to be much smaller than that used on the Chalais-Meudon model.

CONCLUSIONS

The foregoing results demonstrate the effectiveness of boundary-layer control on a wing of pronounced sweep and whose basic profile is comparatively thin.

They show, moreover, that the source of energy used, bleeding off from a turbojet, results in a significant energy balance since the thrust loss is negligible at take-off and enables landings in sensibly horizontal steady state.

The summary numerical applications merely prove that different numbers of injectors must be used at take-off and landing, such as two rows of injectors, for example, one for take-off, both for landing.

A study under way on suction at shock wave level, on airfoil SO 6008 bis, zero incidence, has proved the complete absence of break-away for extremely small suction flows.

It seems justifiable to elaborate the study of the solution by ejectors and flat mixers. A much greater control efficiency and simple design should be attainable, since the mixer is reduced to two flat surfaces.

The lateral control should be examined correlatively with the high-lift devices. The efficiency of a differential aileron setting should be checked, an efficiency which appears attained, since precisely the flow over the flap α_2 is correct, even at high incidence.

Lateral control by differential injection might be explored.

Such studies have been scheduled in the supplementary program on the Chalais-Meudon model.

Although the work at Chalais-Meudon was made on a full-scale wing, with corresponding limitations, it should be pointed out that only laboratory studies are involved, and that the application of boundary-layer control by bleeding off from the turbojet poses technical and structural problems which are outside the scope of the present research program.

Translated by J. Vanier
National Advisory Committee
for Aeronautics

REFERENCES

1. Poisson-Quinton: Idées nouvelles sur le contrôle de la couche limite appliqué aux ailes d'avion. Les Cahiers d'Aérodynamique, no. 3, 1945.

Deplante: Hypersustentation, commandes Transversales. Technique et Science Aéronautique, no. 2, 1946.

2. Sedillé: La propulsion par réaction en combinaison avec l'aspiration de la couche limite. Ier Congrès National de l'Aviation, 1945.

3. Dupin et Morain: L'alimentation en air des turbo-réacteurs par aspiration de la couche limite. Technique et Science Aéronautiques, no. 5, 1947.

4. Poisson-Quinton: Recherches théoriques et expérimentales sur le contrôle de la couche limite. VIIe Congrès International de Mécanique Appliquée, Londres, septembre 1948.

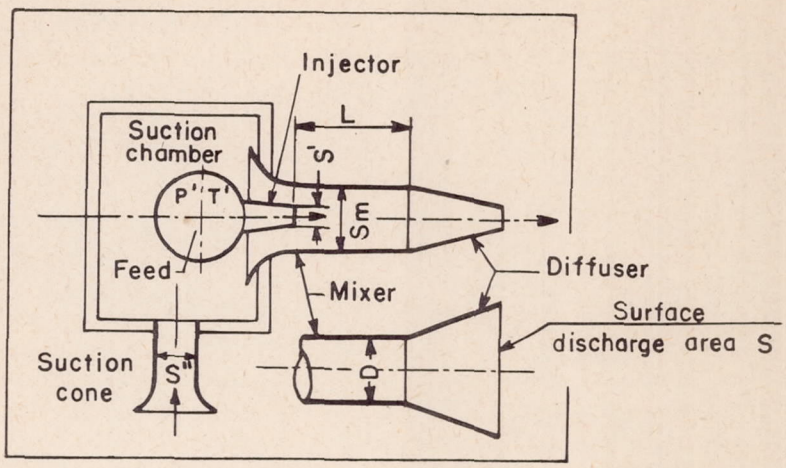

Figure 1.- Test setup of ejector.

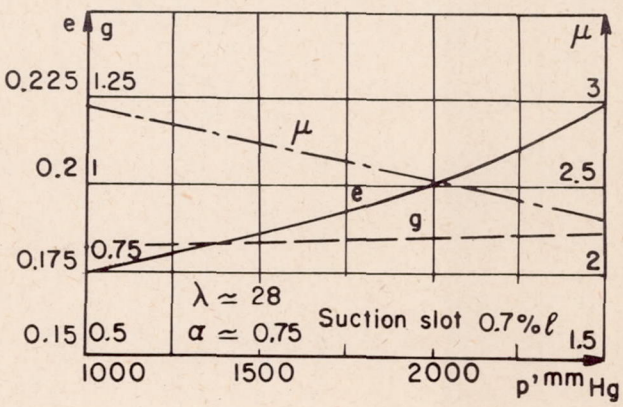

Figure 2.- Parameter of operation of the ejector units used on the S.O. 6020 wing.

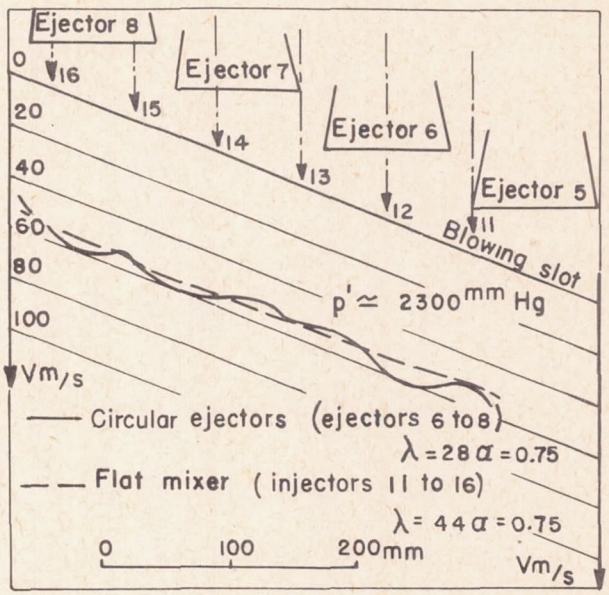

Figure 3.- Spanwise distribution of blowing jet.

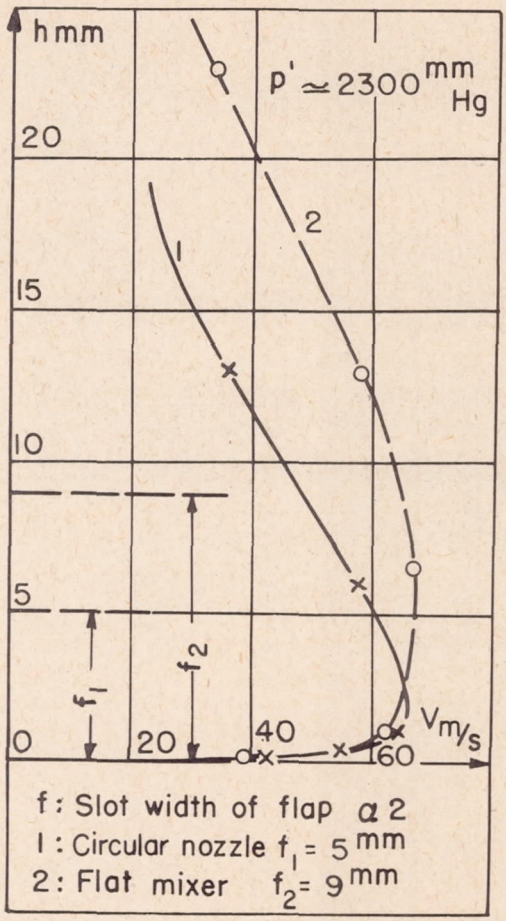

Figure 4.- Velocity profile 100 mm downstream from blowing slot.

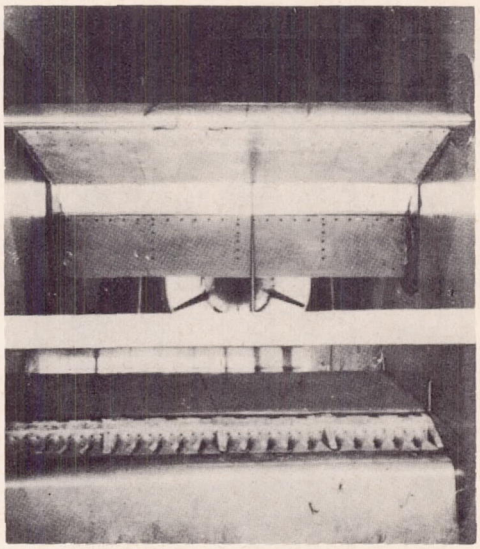

Figure 5.- Metal model; view of inside, cover of flap α_1 has been removed.

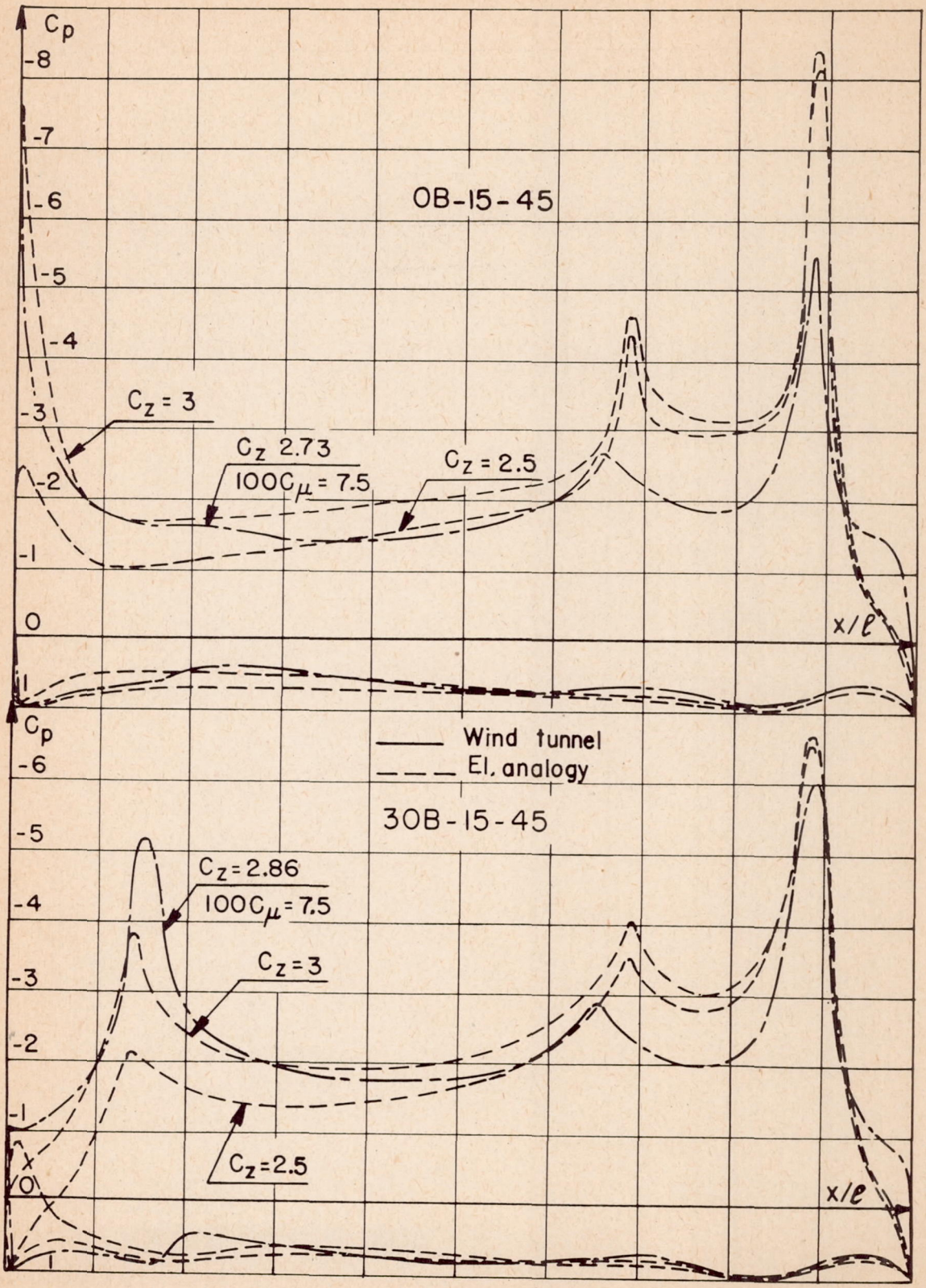

Figure 6.- Comparison of theoretical and experimental pressure.

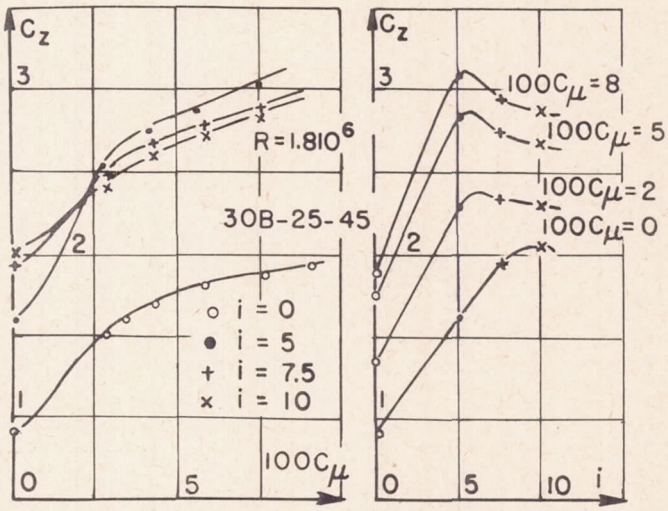

Figure 7.- Example of high-lift device in two-dimensional flow.

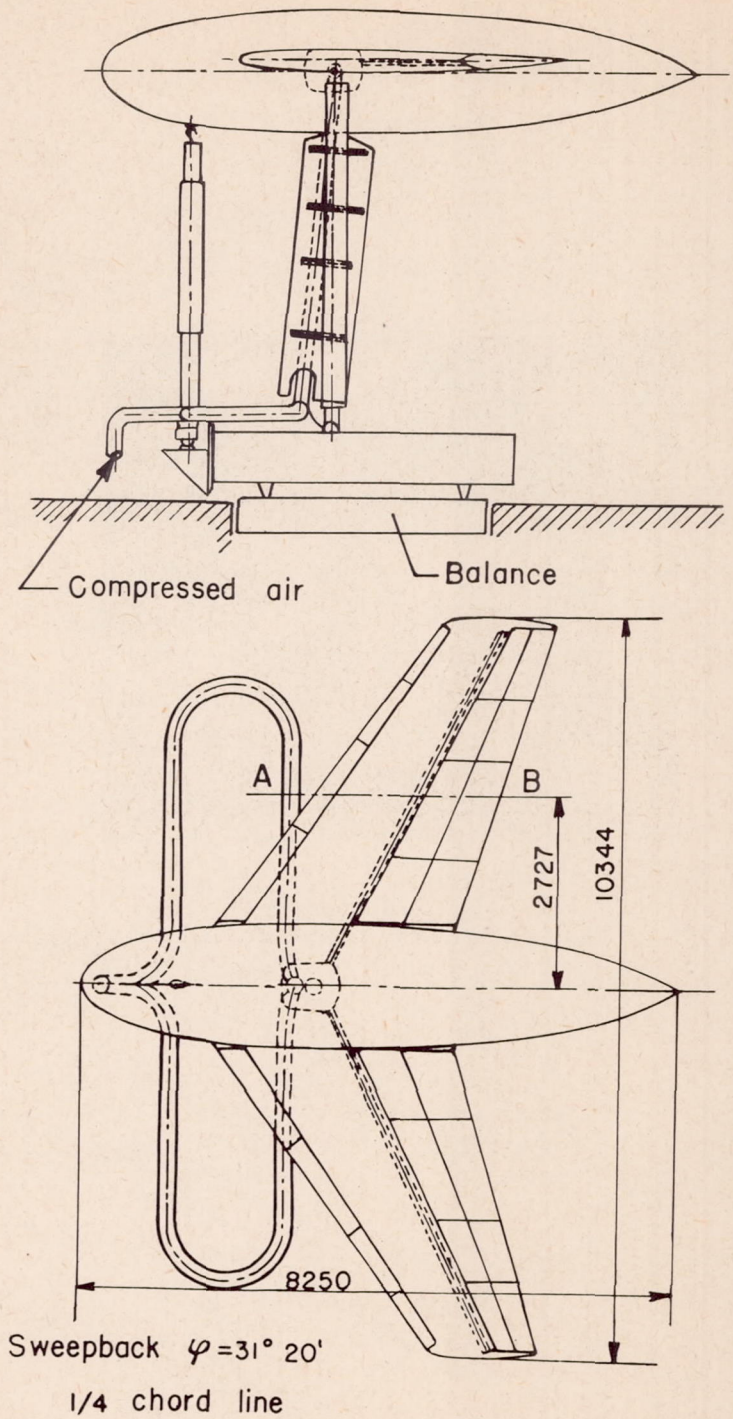

Figure 8.- Model S.O. 6020.

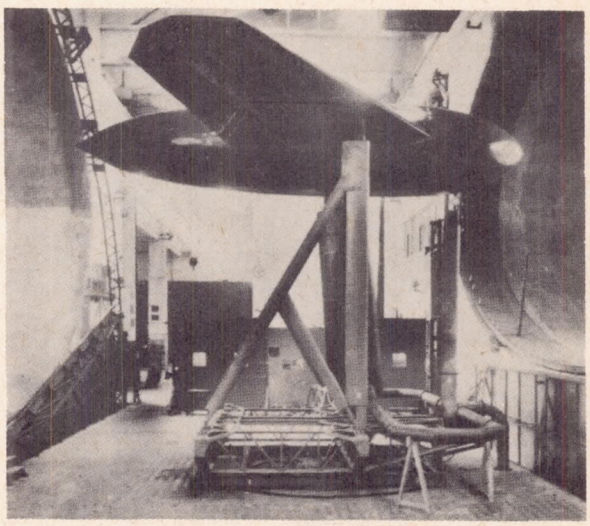

Figure 9.- Setup in large tunnel at Chalais-Meudon.

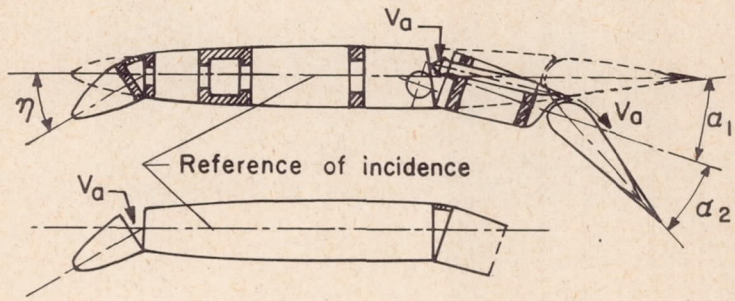

Figure 10.- Section of profile: suction from first flap or the leading edge.

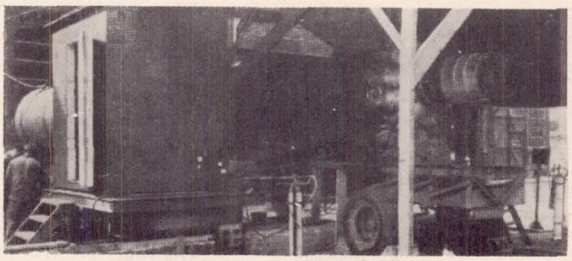

Figure 11.- Turbojet and control cabin.

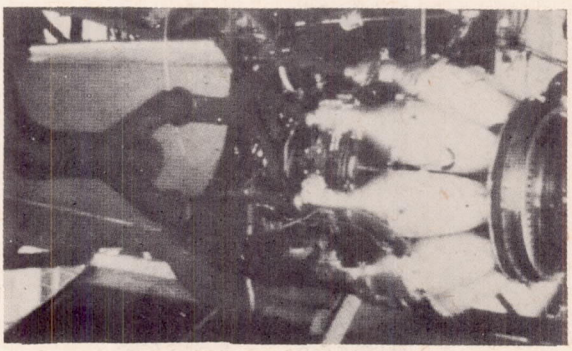

Figure 12.- Bleeding off air from turbojet.

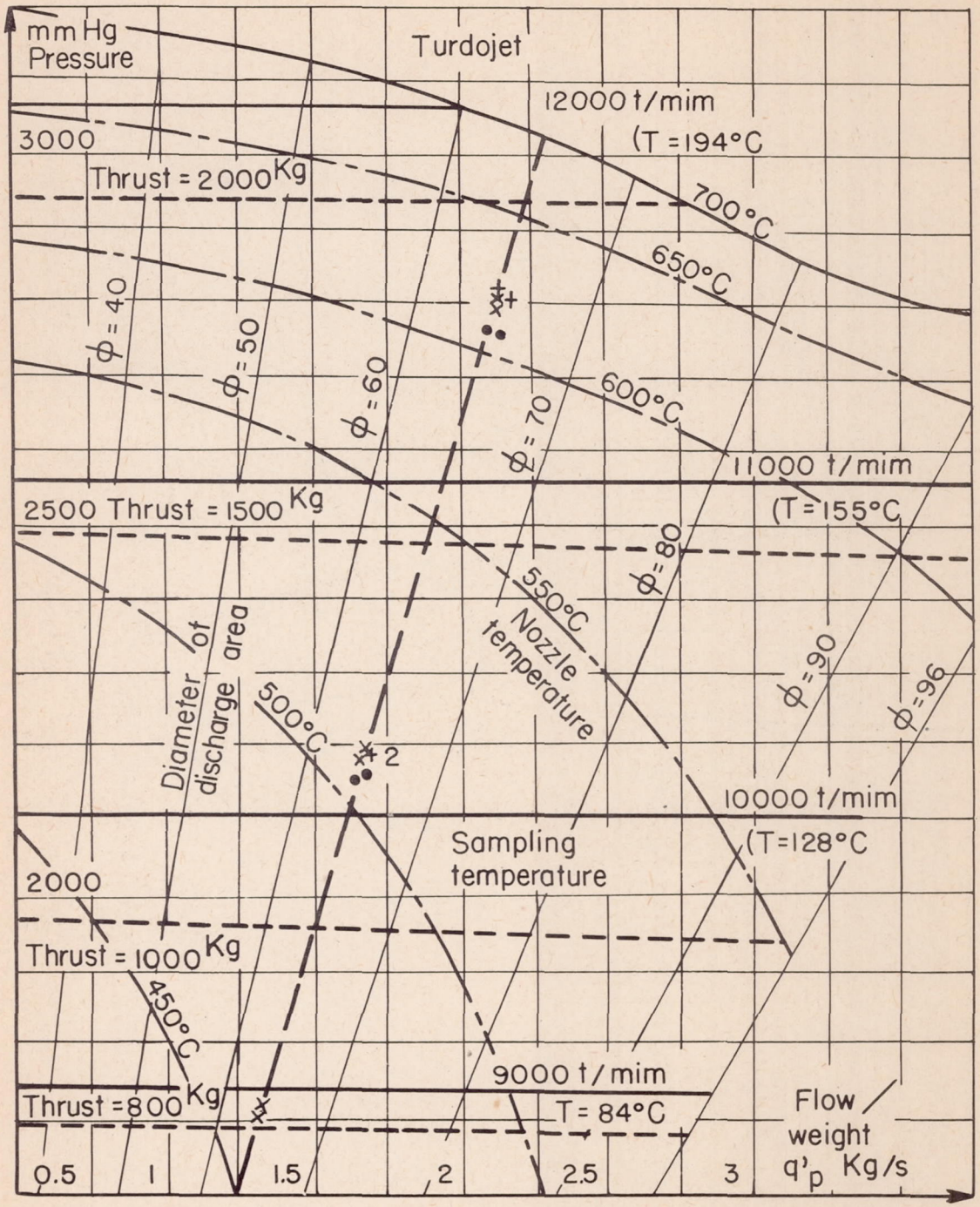

Figure 13.- Characteristics of Hispano-Suiza Nene turbojet operation with bleed-off.

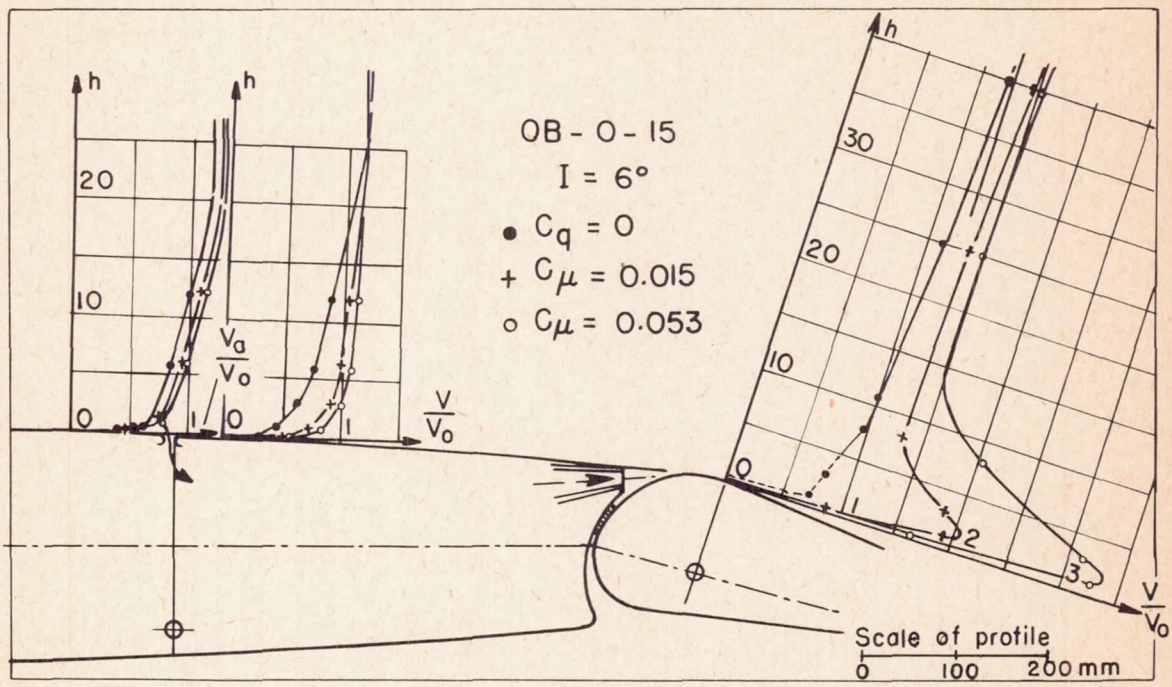

Figure 14.- Velocity profile adjacent to suction and blowing slots.

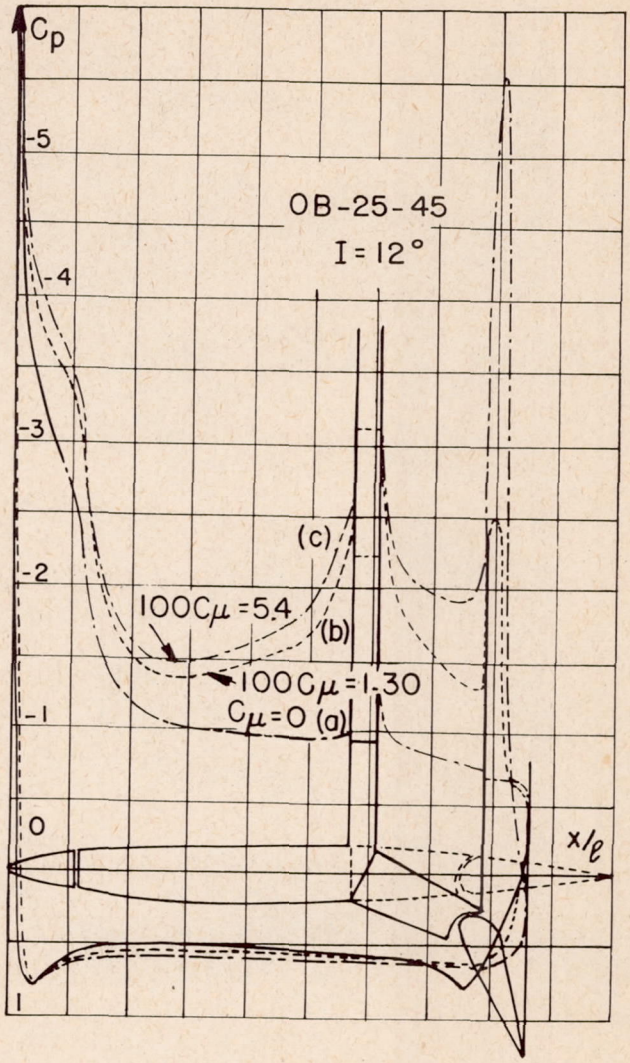

Figure 15.- Experimental pressure, section AB of wing.

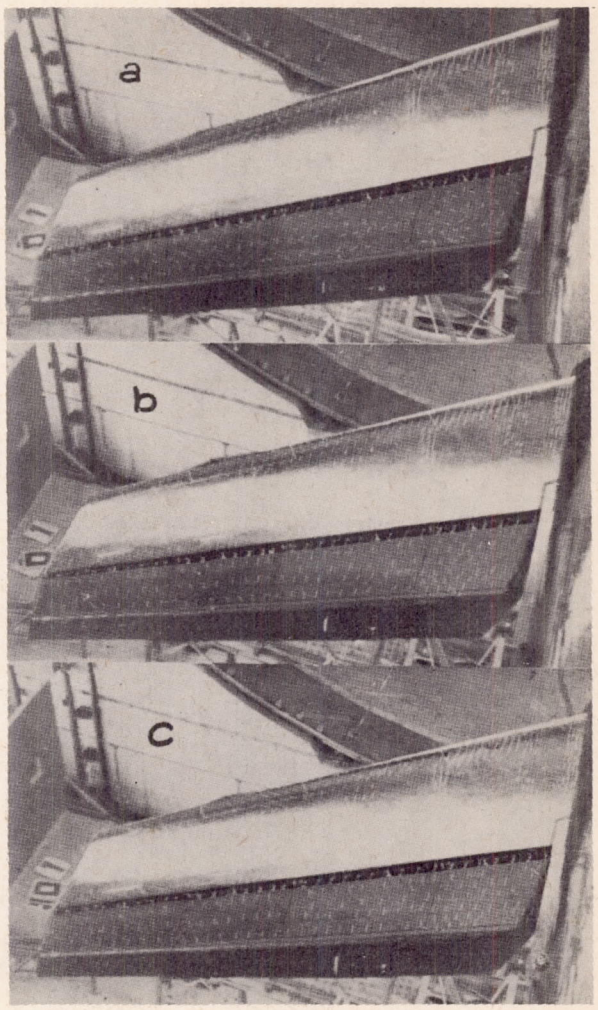

Figure 16.- Visualization: (a) flaps separated, (b)α_1 partially separated, (c)α_1 and α_2 readhering.

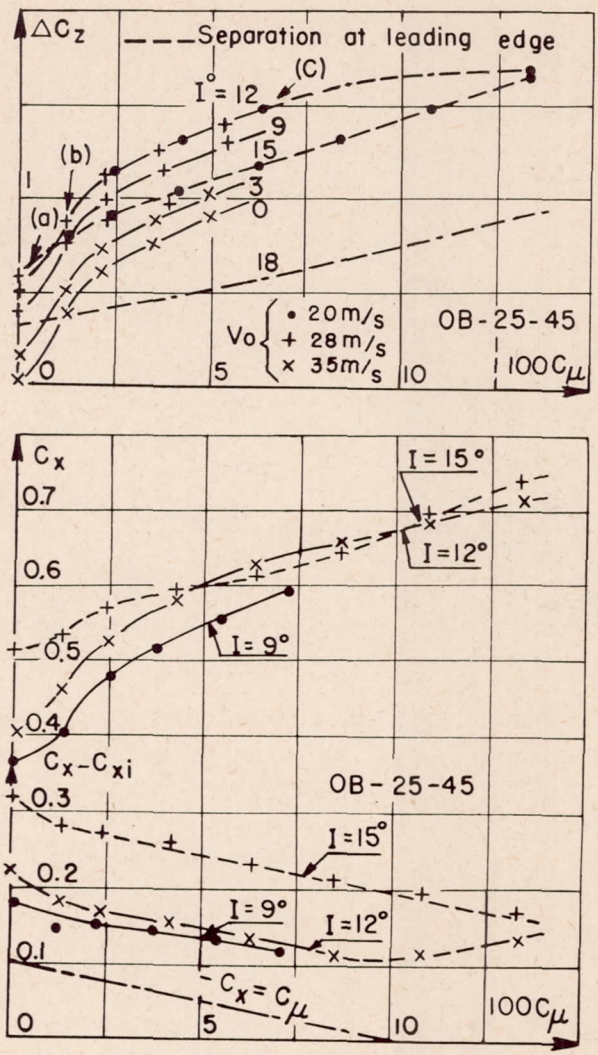

Figure 17.- Evolution of lift and drag with C_μ.

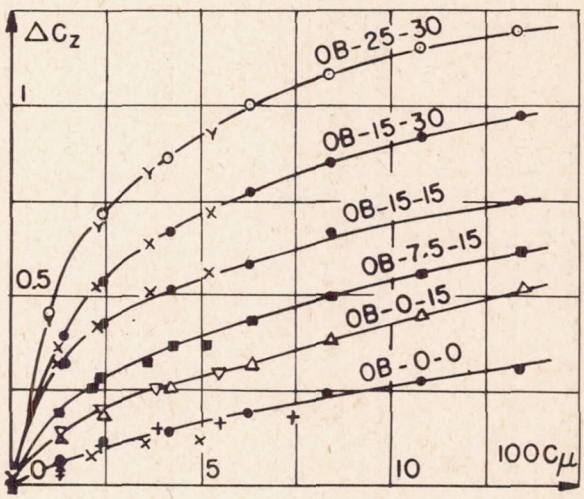

Figure 18.- Effect of flap setting on the C_μ of readherence.

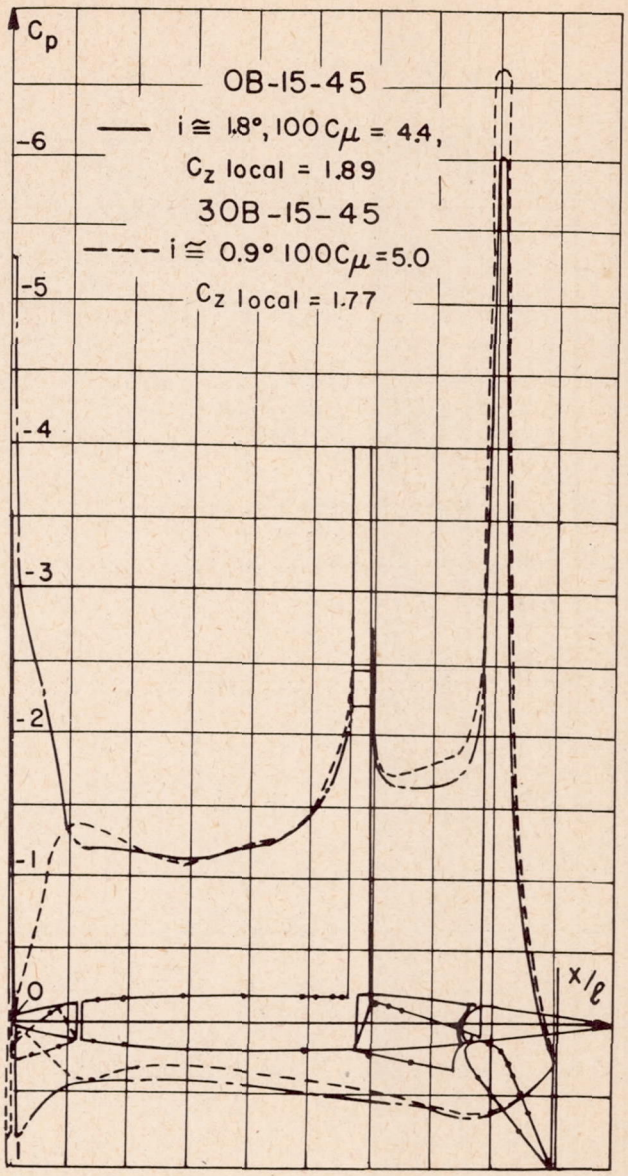

Figure 19.- Effect of drooped nose.

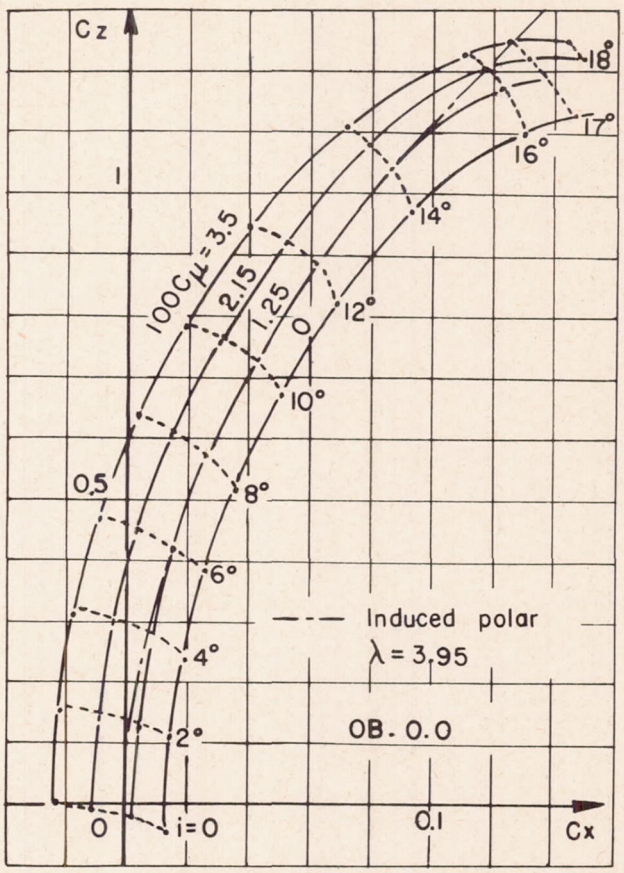

Figure 20.- Flap polar not set.

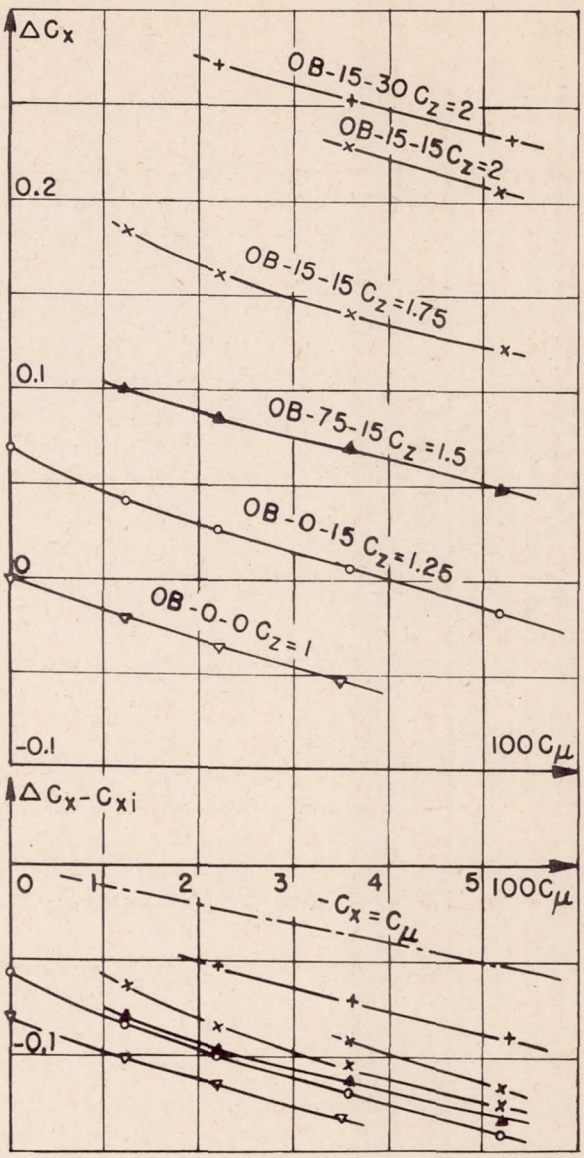

Figure 21.- Comparison of take-off configurations.

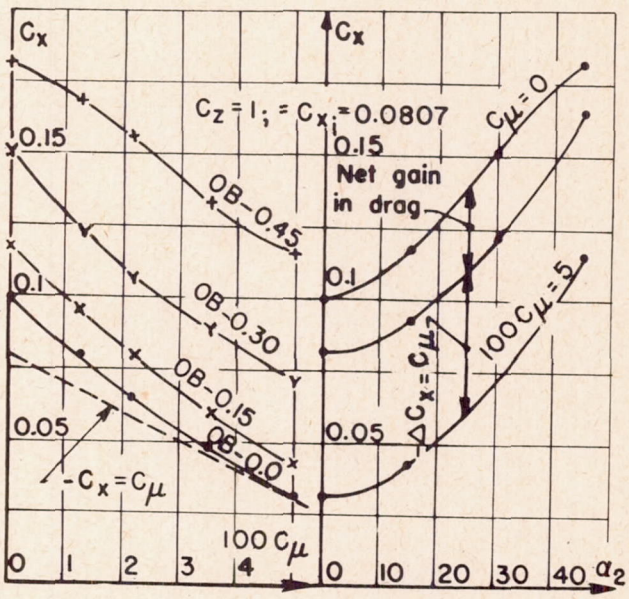

Figure 22.- Effect of blowing flap setting on drag.

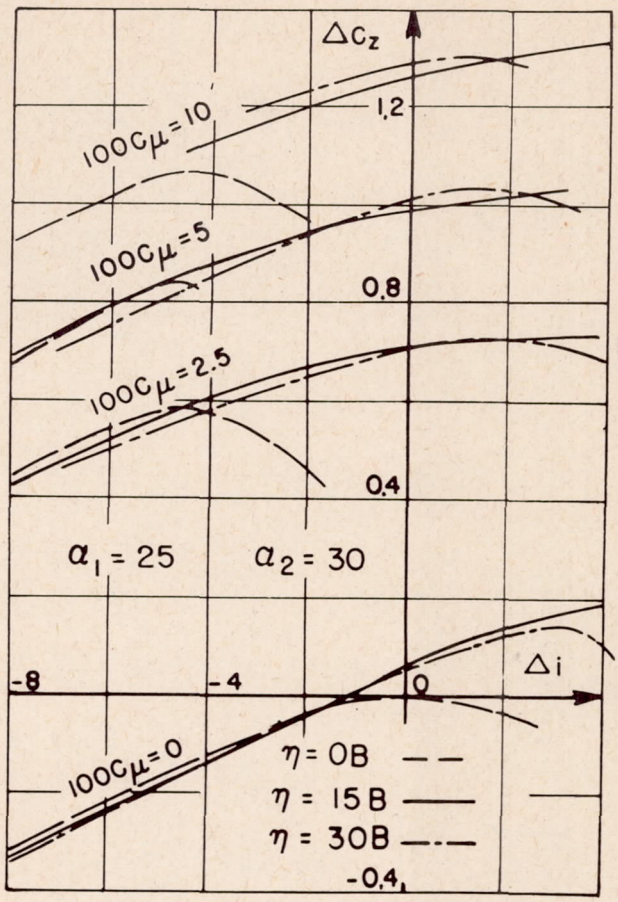

Figure 23.- Effect of drooped nose η.

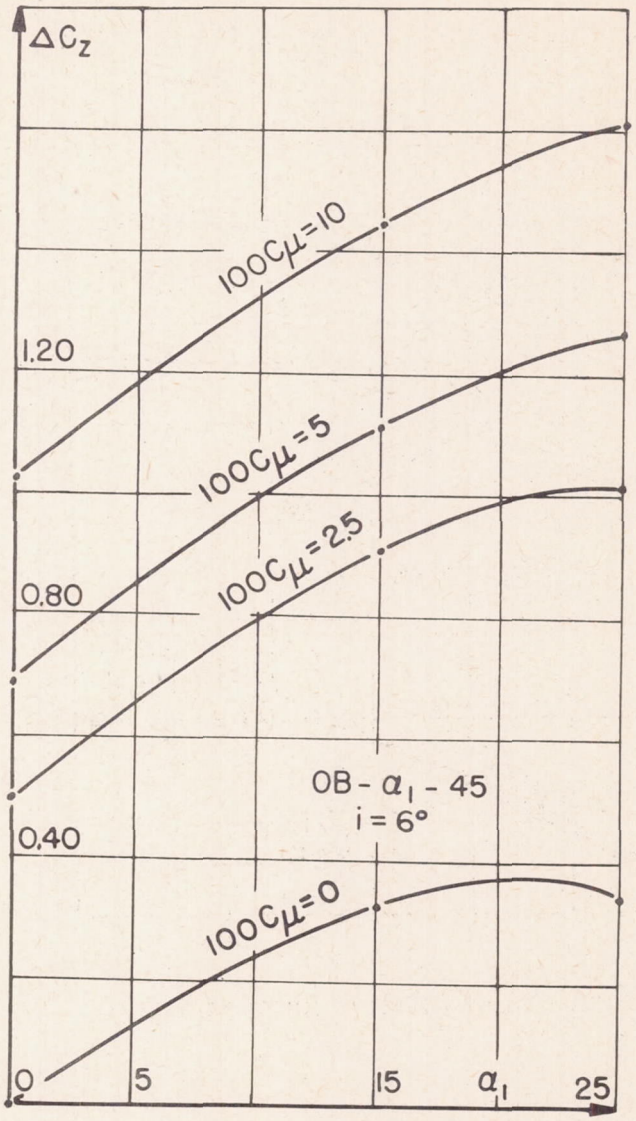

Figure 24.- Effect of suction flap setting α_1.

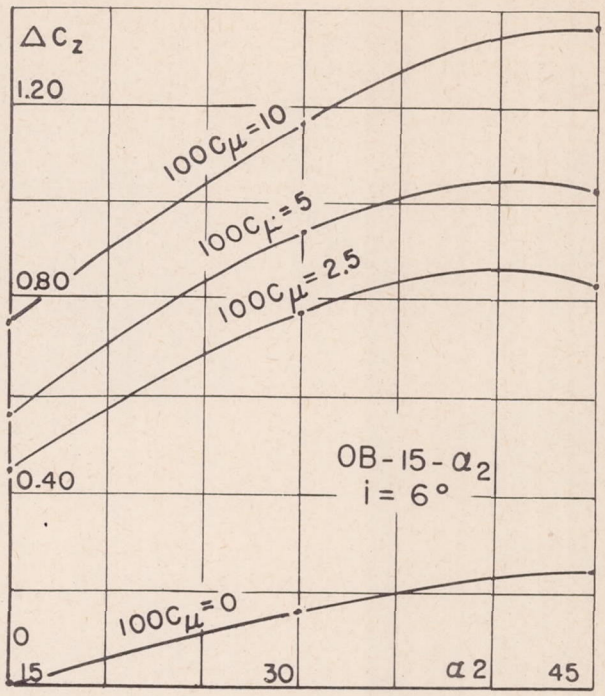

Figure 25.- Effect of suction flap setting α_2.

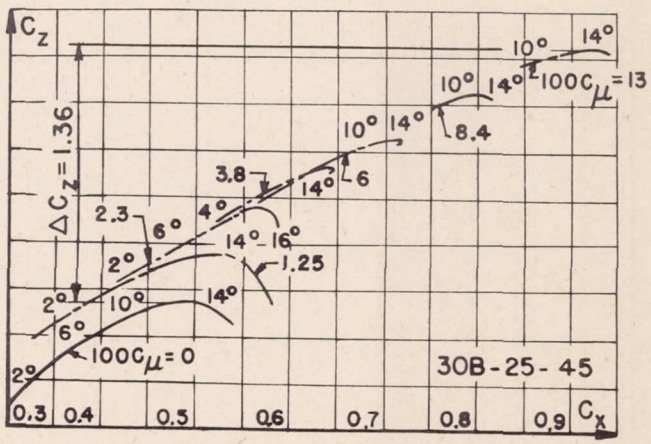

Figure 26.- Family of polars for a landing configuration.